Journal of the Korean Geo-Environmental Society
23(1): 15～23. (January 2022) http://www.kges.or.kr

ISSN 1598-0820 (Print)
ISSN 2714-1233 (Online)
DOI https://doi.org/10.14481/jkges.2022.23.1.15

Simple Evaluation Method of Uplift Resistance for Frictional Shallow Anchors in Rock

Daehong Kim† · Seungho Lee[1)]

Received: October 29th, 2021; Revised: November 4th, 2021; Accepted: December 7th, 2021

ABSTRACT : This paper presents the results of full-scale load tests performed frictional anchors to various lengths at several sites in Korea. Various rock types were tested, ranging from highly weathered shale to sound gneiss. In many tests, rock failure was reached and the ultimate loads were recorded along with observations of the shape and extent of the failure surface. Laboratory tests were also conducted to investigate the influence of the corrosion protection sheath on the bond strength. Based on test results, the main parameters governing the uplift capacity of the rock anchor system were determined. By evaluation of the ultimate uplift capacity of anchor foundations in a wide range of in situ rock masses, rock classification suitable for structural foundation was developed. Finally, a very simple and economical design procedure is proposed for rock anchor foundations subjected to uplift tensile loads.

Keywords : Failure mechanism, Frictional anchor, Bond strength, Uplift behavior

1. Introduction

Design of rock anchor foundations requires specifications of the diameter, length, and spacing of the individual anchors. These design parameters are normally determined so as to insure the overall stability of foundations considering the nature of the surrounding rock mass, the allowable displacements, and the risk of tendon corrosion. In order to assess the overall safety factors for the anchored foundations, the following failure modes (Xanthakos, 1991) must be examined:

(a) Structural failure of steel tendon
(b) Bond failure at tendon/grout interface
(c) Shear failure at grout/rock interface
(d) Rock pull-up failure

The stability of a rock anchor system is related to the volume of rock mass mobilized to resist the uplift force. The shape of such failure volume is commonly assumed as an inverted cone with its apex at the top, middle or bottom of the fixed anchor and an included angle of 60° or 90° depending on the rock type (Littlejohn & Bruce, 1977). Then, the embedment depth is obtained by equating the applied load either to the weight of failure volume or to the shearing strength mobilized on the conical failure surface.

Dados (1985) completed a series of ten field pullout tests on vertically cemented rock anchors installed in “unweathered granite”, with “moderately” spaced sub-horizontal jointing. The testing results indicated that as the pullout load increases the rock bulges upward to a distance roughly equal to the anchor depth. The author also described the simultaneous formation of tension cracks along the joints and separation of blocks along the sub-horizontal jointing observed on site. Dados suggested an empirical relationship for the site which suggested that “the pullout capacity of a certain anchor in a certain discontinuous rock can be estimated based on empirical values from past experience of the probable total anchor deflection at failure”. Observations from this author are consistent with Bruce (1976) that the rock mass dilates or deforms in a progressive manner prior to ultimate failure or “cone pullout”.

The testing completed by Carter was consistent with the results of Saliman and Shaefer (1968) and Ismael (1982) which suggest that the dead weight cone approach is conservative, however, Carter (1995) concluded while the testing was very valuable for assessing the response of the rock mass at the site, the absolute results are not widely applicable beyond the site. Carter noted that although nearly all of the tests that have been reported in the literature suggest that basing ultimate capacity on dead cone weight is conservative, not

† Vice-president (Ph.D/P.E.), Jungang Research Institute of Safety and Technology (Corresponding Author : dhkim2121@daum.net)
1) Professor (Ph.D/P.E.), Dept. of Civil Engineering, Sangji University

enough information is yet available to formulate an effective alternative. Carter also concludes that "obviously, more site testing of cone failure mechanisms is essential if current design approaches are to be rationally improved." Since the work of Carter, attempts have been made to correlate the behaviour of the rock mass to RQD and RMR.

Recently, Thomas-Lepine (2014) completed testing of approximately 50 bolts embedded 0.5-1.5 m into rock. The author identified that the discrete location of fractures in the rock mass have an influence on the failure mechanism of the anchor. Thomas-Lepine, identified two failure mechanisms for anchor pullout including "liberation of a block" and "generalized cracking", and photos of these failure mechanisms is presented in this research. The work by this author also identified that variation exists in the rock mass across a site. You & Lee (2017) performed the pull-out resistance behavior of the anchor with the bump type resistors at the anchor body was experimentally investigated. As a result, the pull-out behavior of the friction type anchor and the expansion type anchor was different. As the number of resistor increased, the maximum pull-out resistance increased and the residual pull-out resistance ratio increased significantly, which were at 171～591 percent larger than that of the friction type anchor.

In this study, we performed a large number of extensive full scale field tests as well as small scale laboratory tests in order to develop a practical and economical design method. From a detailed analysis of the test results, we have determined the main parameters governing the uplift capacity of rock anchor systems. By evaluating the ultimate uplift capacity of anchor foundations in a wide range of in situ rock masses. In particular, a number of full scale group anchor tests demonstrated the practical applicability of rock anchor foundations.

Laboratory tests were also performed to investigate the influence of a corrosion protection sheath on the bond strength at the tendon/grout interface when the sheath is installed in cement-based grout.

2. Laboratory tests for bond failure Evaluation of anchor-grout interface

2.1 Test set-up

The present laboratory pullout tests were conducted to determine bond strength and bond stress-shear slip relation at the tendon/grout interface when a corrosion protection sheath is installed in the cement-based grout. Two different anchor types were considered in these tests, as shown in Table 1. The first type is conventional deformed reinforcing bar (hereafter called "rebar") with diameters of 32 mm and 51 mm. The second type is strong Macalloy steel thread bars (hereafter called "thread bar") with diameters of 36 mm and 50 mm. These anchors were inserted in cement grout contained in irregularly surfaced rigid steel cylinders.

As shown in Figure 1, two different anchor models were considered in the present tests. Model (a) was used to find the bond stress-slip relation along the tendon/grout interface. A relatively short embedment length was used to assure a uniform bond stress distribution near failure. Model (b) was used to study the bond strength of the tendon/grout interface. These tendons were surrounded by corrugated sheathing to protect against corrosion. Strain gages were installed to measure strains along the protection sheath and tendon/grout interface.

2.2 Results of pullout tests

As typically shown in Figure 2, all pullout tests revealed

Table 1. Mechanical properties of anchor and grout types

Anchor types			Yield force (kN)	Compressive strength of grout after 7 days (MPa)
Rebar	SD40-D32	A	305~400	34.3
	SD40-D51	B	770~1011	34.3
Thread bar	36-mm	C	863	34.3
	50-mm	D	1665	34.3

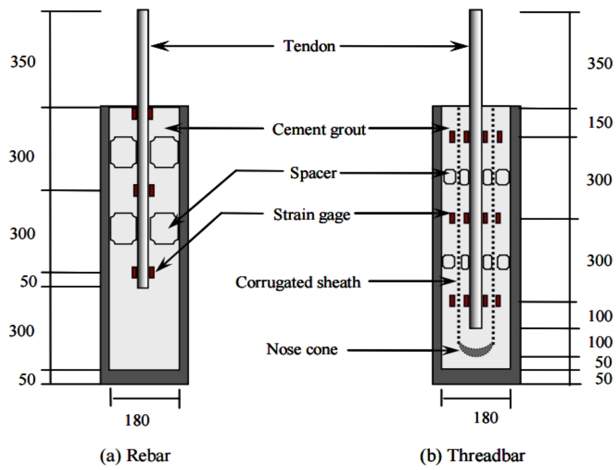

Fig. 1. Anchor models tested (unit: mm)

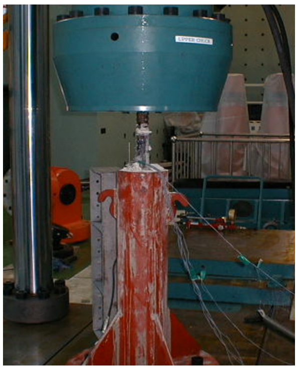

Fig. 2. Tendon-grout bond failure

shear failure at the tendon/grout interface. The shear bond strengths at the interface are mainly due to mechanical interlocking and friction associated with movement of the tendons relative to the surrounding grout. Test results supported the following empirical equation relating the ultimate bond strength (τ) to the unconfined compressive strength of grout (f'_c) as

$$\tau = \alpha \cdot f'_c \tag{1}$$

where the constant α was found to be 18.5±4% for the rebar and 21.5±4% for the thread bar. Thus, the Macalloy thread bars have approximately 16% higher bond strength than the conventional reinforcing bars. The bond strength between tendon-grout shows a larger value for Macalloy bars, which is thought to be because the roughness of Macalloy bars is larger than that of rebars and the pitch spacing is also tight.

It should be noted that Equation (1) is obtained at grout unconfined compressive strength of 34.3 MPa. One of the important findings from these tests is that the measured strains along the corrosion protection sheath were so small that practically the reduction of bond strength by the presence of sheath would be negligible.

Figure 3 shows load-displacement curves obtained from the pullout tests. The load-displacement relations of rebar can be characterized by three distinctive stages. The first stage is related to elastic behavior approximated by a straight line. The second stage is associated with elasto-plastic behavior reaching the ultimate strength. The last stage is related to softening behavior due to progressive debonding, which will eventually approach the residual strength. During the loading stages, the Macalloy thread bars show higher strengths than the conventional rebar. However, as the debonding is completed, both types of anchors reach essentially the same residual strength.

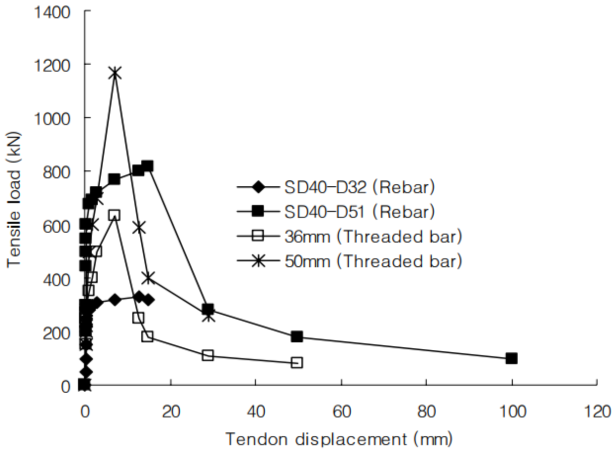

Fig. 3. Load-displacement curves by pullout tests

3. Full scale field tests

3.1 Test sites and characteristics of rock anchors

Full scale field tests were performed, at three different locations (Taean and Okchun in Chungcheong Province and Changnyong in Gyeongsang Province). Static pullout tests were conducted for 54 passive rock anchors and 4 anchored footings. In the majority of test sites, flat bed rocks are exposed on the ground surface. To determine the properties of in situ rock mass, 34 rock cores of NX-size were obtained from drilled boreholes in the vicinity of the test sites. The rock cores show some fractures and horizontal thin beds ranging in thickness from 30～200 mm within a depth of 1～5 m.

Table 2 shows geometrical and mechanical properties of the rock mass obtained from these rock core samples. Note that the values of compressive strength represent the unconfined compressive strengths conducted on intact core samples.

Reinforcing steel rods (rebar) used for anchors have a nominal diameter of 32 mm and 51 mm. These steel bars have an elastic limit of 384～504 MPa and an ultimate strength of 553 MPa. A hydraulic crawler drilling machine was used to make 100 mm diameter holes. Anchors were inserted into the holes with cement grout to their full length varying between 1 m and 6 m and pullout tests were then performed

Table 2. Geometrical and mechanical properties of the rock

Testing sites	Taean		Changnyong		Okchun
	Hole No. (TA-1)	Hole No. (TA-4)	Hole No. (CY-2)	Hole No. (CY-3)	Hole No. (OC-5)
Rock type	Gneiss	Gneiss	Shale	Shale	Limestone
Core recovery (%)	93	69	75	40	86
R.Q.D. (%)	84	32	26	10	50
Unit weight (KN/m³)	29.3	27.6	25.9	26.1	28.6
Poisson's ratio	0.22	0.23	0.20	0.23	0.23
Modulus of elasticity (GPa)	69.8	63.4	62.3	65.6	74.7
Compressive strength (MPa)	112.3	105.6	110.4	99.8	108.3
Friction angle (degree)	39	37	35	37	43
Cohesion (MPa)	43	38	33	34	38

after the grout was completed. The cement grout was made from Ordinary Portland Cement (OPC) with a water-cement ratio of 0.4. To offset the shrinkage of cement grout, an expansive agent (CONACE AC) at a ratio of 1% by cement weight was added. The compressive strength of the grout at 7 days is 34.3 MPa. Strain gages were installed along the rebars for 3 tests in Taean and 2 tests in Changnyong to measure the variation of strain profiles as the applied load increases.

3.2 Installation and test procedure

Figure 4 and Table 3 show a description of the test setup and installation, respectively, for single rock anchors. As shown in Table 3, single rock anchors were installed over a wide range of rock types and qualities with a fixed anchored depth of 1~6 m. The majority of installations used 51 mm high grade steel rebar to induce rock failure prior to rod failure.

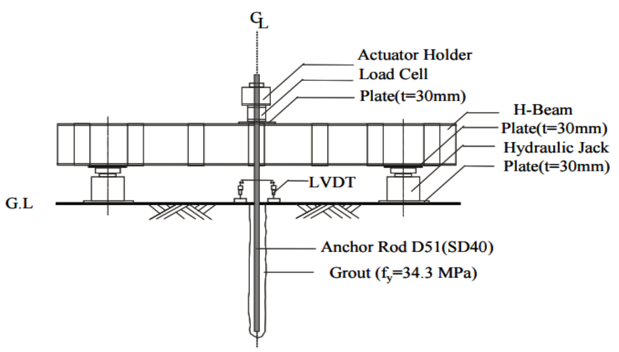

Fig. 4. Test setup for a single rock anchor

Table 3. Installation of single rock anchors

Depth (m)	Metamorphic rock (Taean)				Sedimentary rock (Changnyong)	Metamorphic rock (Okchun)	Total
	H	M	S	Sub total	M	M	
1.0	2	4	3	9	-	1	10
1.5	1	-	1	2	2	-	4
2.0	3	4	2	9	3	4 (D=32mm)	16
2.5	-	-	2	2	-	2 (D=32mm)	4
2.6	-	1	-	1	-	-	1
3.0	3	3	-	6	4	2 (D=32mm)	12
3.7	-	-	-	-	3	-	3
4.0	1	-	-	1	-	-	1
5.0	-	-	-	-	-	2 (D=32mm)	2
6.0	-	-	-	-	-	1 (D=32mm)	1
Total	10	12	8	30	12	12	54

(H: Highly weathered, M: Moderately weathered, S: Slightly weathered rock)

However, a few installations included the use of 32 mm rebar at relatively deeper anchored depth so as to induce rod failure.

Table 4 and Figure 5 show a description of the test setup and installation, respectively, for group anchored foundations. The main objective of these full scale tests is to demonstrate the practical applicability of rock anchor foundations subjected to the design uplift load. As illustrated in Table 4, group anchors consisting of 8 holes with anchored depth of 2 m and 5 m were tied to the square foundations (2.5 m × 2.5 m) with depths of 0.8, 1.0 and 1.2 m. Two 32 mm rebars were inserted into each hole.

Fig. 5. Test setup and layout for a group anchor (unit: m)

Table 4. Installation of group rock anchored-foundation

No.	Dim. of foundation (m)	Anchor hole		Tendon (each hole) (SD40-D32)	Depth (m)	Location
		Dia. (mm)	No. of Hole			
1	2.5x2.5x1.2	100	8	2	5.0	Okchun
2	2.5x2.5x1.0	100	8	2	5.0	Okchun
3	2.5x2.5x0.8	100	8	2	5.0	Changnyong
4	2.5x2.5x1.0	100	8	2	2.0	Changnyong

As shown in Figures 4 and 5, hydraulic jacks were used to apply the vertical uplift loads. Although the maximum loads can reach up to the failure of the rock anchor system, current tests were terminated at 95% of the yield strength or 80% of the ultimate strength of the steel rods to secure the safety of personnel and to prevent equipment damage. When some parts of the anchors failed before the permitted load, the causes of failure were investigated along with the diagnosis.

Table 5 shows the load increments in terms of the percent of f_u, where f_u stands for the ultimate strength of rebars, along with the minimum period of observations. Load-displacement data were plotted continuously over a range of 5% to 80% of the ultimate strength (f_u) of the rebars with each load increment not greater than 10% of the ultimate strength.

During unloading, displacements were measured at one-third points of the peak load which was occurred in that cycle. For each stage, loading was held for at least 3 min and the corresponding displacement was recorded at the beginning and end of each period. At peak loads for each cycle, loading was held for at least 15 min. with an intermediate displacement reading every 5 min. The seating load was considered as the initial load when the initial seating load is greater than 5% of the ultimate strength of the rebar, and thereafter as datum when cyclic loading is performed. Where appropriate, the final load cycle was repeated to check the reproducibility of the load-displacement curves. The uplift movements along the anchors and grout/rock interface were measured by strain gages attached to the long steel bars.

3.3 Single anchor

The present test results for single anchors show the bond failures along the interface between grout and rock in the case of very shallow anchor depths of 1~1.5 m in highly weathered rock (Figure 6) and the rock pull-up failures in the case of fresh, sound rocks or deeply embedded rock anchors. According to the test results, rock-grout bond failure is governed by the rock conditions and the average bond failure is 10~12% of the unconfined compressive strength of the surrounding rocks as shown in Table 6. Bond failure along the interface between the rod and grout was not observed throughout the present tests. For the majority of rock pull-up failures, cracking and heaving on the ground surface were extended radially to a distance equal to the half depth of the anchor, as shown in Figure 7.

Test sites in the city of Taean are classified as metamorphic gneiss, which covers a wide range of rock conditions. Test results revealed an uplift capacity ranging from 150 kN to 940 kN, which depends mostly on the embedded length, RQD (Rock Quality Designation), and core recovery. As the failure of the rock mass was reached, "+" shape cracks developed around the anchor and extended radially. Readings from strain gages installed in moderately weathered rocks along the depth showed a large strain increase at the half depth as the applied load is reached to failures. These test results showed the extent of cracking on the ground surface which is about the half embedded depth.

Bond failures between the grout and rock were observed for the anchors with a fixed length of less than 1.5 m, embedded in low RQD rocks.

Test sites in the city of Changnyong are classified as sedimentary shale with a RQD of 0~30% and a core recovery

Table 5. Load increments and minimum periods of observation for proving tests

Load increments (%, f_u)							Minimum period of Observation (minutes)
Order of cycle							
1st	2nd	3rd	4th	5th	6th	7th and 8th	
5	5	5	5	5	5	5	3
10	20	30	40	50	60	70	3
15	25	35	45	55	65	75	3
20	30	40	50	60	70	80	15
15	20	30	40	40	50	50	3
10	10	15	20	20	30	30	3
5	5	5	5	5	5	5	3

Fig. 6. Rock–grout bond failure (Highly weathered, depth =1.0m)

Fig. 7. Rock failure (Moderately weathered, depth=2.0m)

Table 6. Rock–grout bond failures at Taean

Test No.	Depth (m)	Tensile load at failure (kN)	Hole diameter (mm)
4	1.0	350	100
5	1.0	420	100
6	1.5	680	100

of 34～73%. The rock masses were so weak that they could be separated by hand, with substantial horizontal discontinuities. Though the rocks are of very poor quality, it showed an uplift capacity of over 700 kN in the case where the fixed anchor depth was over 3 m. As the applied load reached the uplift capacity of the rock mass, the rock surfaces were pulled up with many small cracks around the anchor. This failure behavior is believed to be due to the separation/loosening of discontinuities associated with the stress concentration on the ground surface around the anchor. Readings from strain gages attached at different depths indicated a sudden large increase of strains at the half length of the fixed anchors as the applied load initiated the rock failure.

Test sites in the city of Okchun are classified as metamorphic limestone with a RQD of 0～52% and a core recovery of 62～96%. Anchor lengths were varied between 1 m and 6 m. The measured uplift capacity of anchors ranged from 300 kN to 350 kN for a single 32mm rebar and from 600 kN to 650 kN for double 32 mm rebars, indicating the yield of rebar prior to rock mass failure. Figure 8 shows a noticeably extended rebar (left one) after the test, compared to the undeformed rebar before test.

Uplift resistances for single anchors are summarized as a function of RQD in Figure 9 (a) and as a function of anchor depth in Figure 9 (b). For test results of Taean and Changnyong, the uplift resistances measured at the same anchor depth generally increase with RQD and these resistances for the rock masses of the same RQD also consistently show an increase with fixed depth of the anchor. For the test sites of Okchun, however, the uplift resistances simply reveal the strength of rebar regardless of the RQD or anchor depth, since the single 32 mm rebar was embedded at sufficient depth to avoid other modes of failure.

Based on the strain readings and the extent of surface cracks

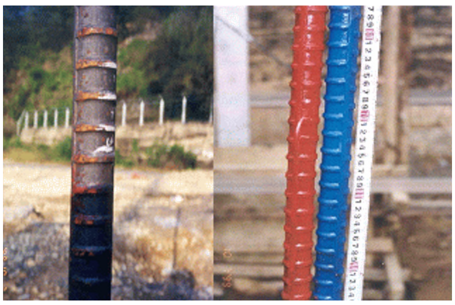

Fig. 8. Rod tensile failure (Moderately weathered, depth=6.0m)

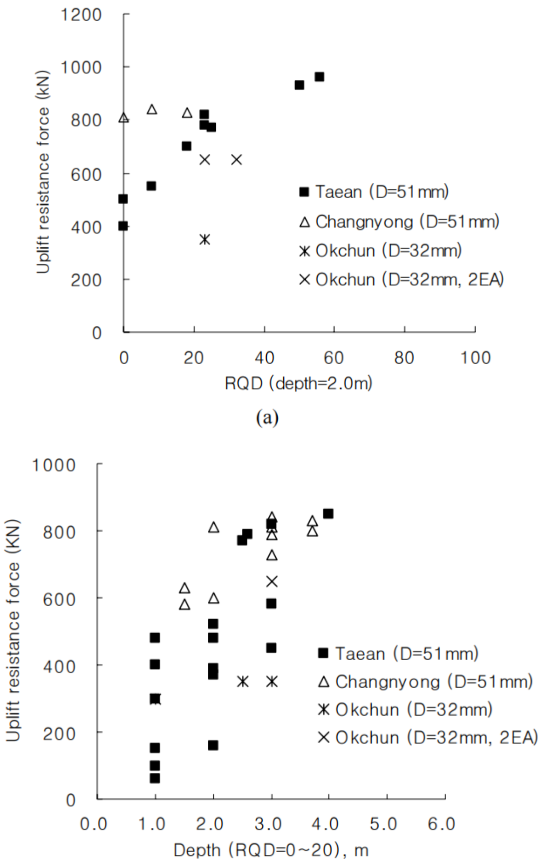

(a)

(b)

Fig. 9. Uplift resistances vs. embedded length and RQD: (a); (b)

at moderately weathered rocks in Taean and Changnyong, the rock pull-up failure was estimated to be an inverted cone with the apex at half the embedded depth and having a contained angle of 90°.

Anchors in poor quality rocks generally fail along the grout/rock interfaces when their depths are very shallow (a fixed length of less than 1.5 m). However, even in such poor rocks, we can induce a more favorable mode of rock pull-up failure by increasing the fixed length of the anchors. On the other hand, anchors in good quality rocks show rock pull-up failures with high uplift resistance even when they are embedded at a shallow depth.

3.4 Group anchor

The group anchor tests were conducted for sites selected based on test results of single anchors such that full size anchored foundations Load-displacement relations of group anchored foundations are presented in Figures 10 (a) and 10 (b) for tests No. 1 and No. 2, respectively, in Okchun, and in Figures 10 (c) and 10 (d) for tests No. 3 and No. 4,

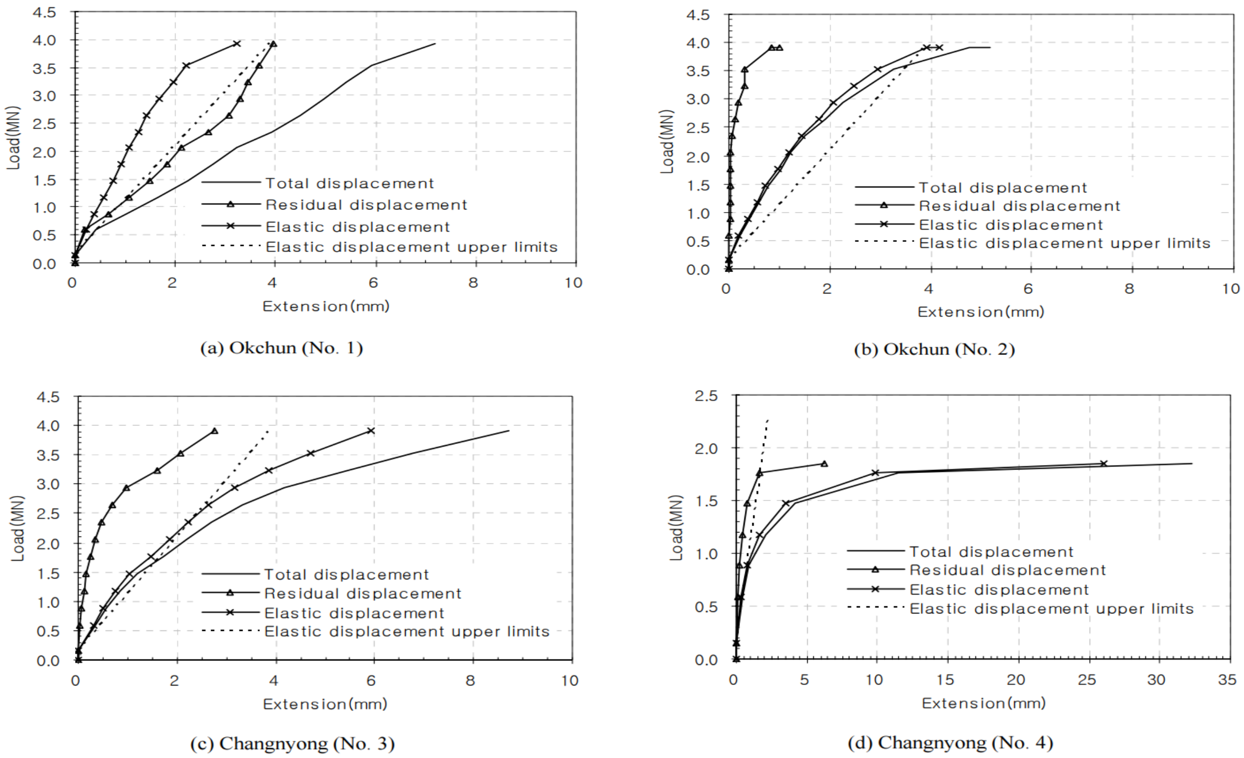

(a) Okchun (No. 1) (b) Okchun (No. 2)

(c) Changnyong (No. 3) (d) Changnyong (No. 4)

Fig. 10. Load–displacement relation of group anchored foundation: (a); (b); (c); (d)

respectively, in Changnyong. Results of tests No. 1, No. 2, and No. 3, having an anchored length of 5 m, show an ultimate uplift capacity of over 4 MN, which can provide a safety factor of more than 3 for a design load of 1.2 MN. However, the result of test No. 4, having a short anchored length of 2 m, shows an ultimate capacity of only 1.5 MN which gives the safety factor of only 1.25. Judging from our test results the anchor length of 3.5 m may be sufficient to provide a safety factor of 3.

As intended, all four test results show the failure of rock mass. Close examination of test No. 1 reveals that there were large cracks developed suddenly around the rebar at an applied load of 3.6 MN, and thereafter the uplift resistance increased gradually until it reached a maximum capacity of 4.6 MN. This measured maximum load of 4.6 MN is approximately equal to the load calculated by the ultimate strength methods (BS 8081, 1989; DIN 4125, 1990), provided that the effective free length is 50 % of the total anchor length, thus supporting our hypothesis of an inverted cone failure surface with its apex at the middle of the anchored depth.

Closely spaced anchors fail as a group due to interference of the adjoining failure surfaces of individual anchors, resulting in an individual anchor efficiency of less than 100%. Thus, the overall capacity of group anchored foundations depends not only on the material properties of the anchor system but also on the spacing and depth of the anchors (Ismael, 1982; Littlejohn, 1992).

Group anchor tests of No. 1 and No. 2 in Okchun revealed the uplift capacity of about 4,000~4,600 kN. On the other hand, single anchor tests in the same sites show the average uplift capacity of about 700~800 kN. Based on such single and group anchor tests, we have derived a curve, as shown in Figure 11, representing the efficiency as a function of the ratio a/R, where a is the anchor spacing and R is half of the embedded anchor depth (l). When the ratio a/R is greater than 2, the individual anchors in a group have an efficiency of 100%. However, it should not be extrapolated below an a/R ratio of 0.4 since group tests were not conducted below this ratio. For the purpose of practical applications, the efficiency

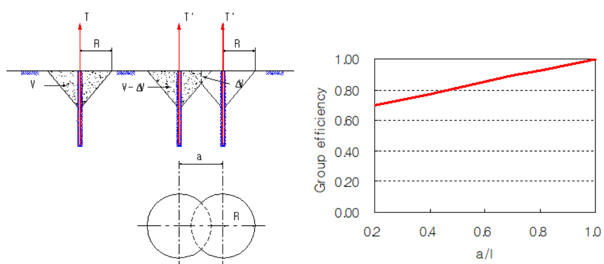

Fig. 11. Group effect of frictional anchor

(β) of an individual bar in group anchored foundations can be approximated by the following linear equation:

$$\beta = 0.375\,(\frac{a}{l}) + 0.625 \quad for\ 0.2 \le \frac{a}{l} \langle 1.0 \tag{1}$$

$$\beta = 1.0 \quad for\ \frac{a}{l} \ge 1.0 \tag{2}$$

where a is the anchor spacing and l is the anchor depth. Note that the above linear efficiency equation uses an anchor depth (l) instead of R on the basis of our inverted cone failure surface with its apex at the middle of anchor depth.

4. Proposed design procedure

Based on our field and laboratory pullout test results, the in situ rock masses are classified into three different classes, as listed in Table 7. Rock anchors must be placed in at least class B rocks with a minimum embedment depth of 3 m.

For the class B rocks with the embedment depth of 3~6 meter and rebar diameter of over 32 mm, our test results show the rock pull-up failures in the form of an inverted cone with its apex at the middle of the embedded depth of the anchor and having a contained angle of 90°. Consequently, the ultimate load of the rock pull-up resistance (T_r) is derived for the individual anchor including the group action effect as

Table 7. Classification of rock masses for frictional anchor

Parameter / Classi-fication	Core recovery	RQD	RMR, Q-Value	Uniaxial compressive strength (MPa)	Elastic wave velocity (km/sec)	Conditions of weathered and discontinuities
A (Good rock)	>70	>25	>70, >10	>80	>3.5	- Slightly weathered - Slightly rough surfaces - Separation <1.0 mm
B (Fair rock)	40~70	10~25	40~70, 1.0~10	50~80	2.5~3.5	- Moderately weathered - Slightly rough surfaces - Separation <1.0 mm
C (Poor rock)	<40	<10	<40, <1.0	<50	<2.5	- Heavy weathered - Slickenside surfaces - Separation 1~3 mm

$$T_r = \beta\left(\frac{\pi l^2}{4\cos 45°}\tau_r + \frac{\pi l^3}{24}\gamma_r\right) \tag{3}$$

where the efficiency (β) is related to the ratio of the anchor spacing (a) and the anchor depth (l) as presented equations (2a) and (2b).

Note that τ_r and γ_r in equation (3) represent the uplift shear strength and the unit weight of the rock masses, respectively. The other less critical failure loads can be computed from the following equations.

For the tendon failure load (T_t):

$$T_t = \sigma_y A_t \tag{4}$$

where σ_y is the tendon strength and A_t is the tendon cross section area.

For the tendon-grout bond failure load (T_{tg}):

$$T_{tg} = \pi D_t \tau_{tg}\ l \tag{5}$$

where D_t is the diameter of the tendon and τ_{tg} is the bond strength of the tendon grout interface.

For the grout-rock bond failure load (T_{gr}):

$$T_{gr} = \pi D_g \tau_{gr}\ l \tag{6}$$

where D_g is the diameter of grout and τ_{gr} is the bond strength of the grout-rock interface.

In order to obtain the optimal incorporation of the in situ rock strength in the design of rock anchor foundations, we assumed that both tendon yield failure and the rock mass pull-up failure occur simultaneously. Based on this concept, the optimum anchor length can be obtained by equating equation (3) to (4) and solving the resultant cubic equation for the given a and l. Then, the number of anchor bars is found so as to satisfy the design uplift load with the appropriate factor of safety. It should be noted that to fulfill this design concept, bond failures at the tendon/grout/rock must be prevented by properly designing the grouted anchors.

The simple design procedure is illustrated in Figure 12 for rock anchored foundations placed in class A or B rocks.

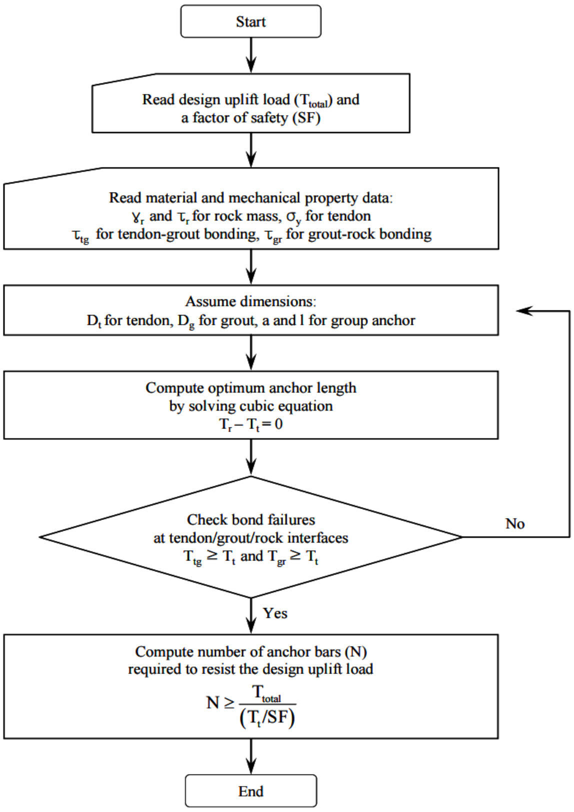

Fig. 12. Proposed design procedure for rock anchor

5. Conclusions

A review of some recent full-scale and laboratory tests carried out for application in structural foundations was presented. From these test results, the uplift capacities and failure modes were evaluated on anchor foundations in various in situ rock masses in several regions in Korea. A rock classification table was thereupon developed. In particular, a number of group anchor tests demonstrated the practical applicability of rock anchor foundations.

Finally, a very simple design procedure is proposed for rock anchor foundations. It is believed that the proposed design procedure can be applied to similar anchored structures where pull-out tensile force is considered to be the dominant load.

Acknowledgments

This work was supported by the Korea Institute of Energy Technology Evaluation and Planning (KETEP) and the Ministry of Trade, Industry & Energy (MOTIE) of the Republic of Korea (No. 20193210100040).

References

1. BS 8081 (1989), British standard code of practice for ground anchorages, British standards Inst., London, England.
2. Bruce, D.A. (1976), The design and performance of pre-stressed rock anchors with particular reference to load transfer mechanisms, Ph.D. Thesis, University of Aberdeen, Scotland, Oct. 1976. Reproduced by EPRI publication (Technical Report No. EL-3777). Load Transfer Mechanisms in Rock Sockets and Anchors. pp 31~42, 142~143, 288-315, 440~454
3. Carter T.G. (1995), Observations on cone pull-out behavior in very weak rock, In Anchors in Theory and Practice, Widmann (ed.), pp. 17~23.
4. Dados (1985), Design of anchors in horizontally jointed rocks, Journal of Geotechnical Engineering, ASCE, 110(11), pp. 1637~1647.
5. DIN 4125 (1990), Ground anchorages - Design, Construction and Testing, German Standards Institution.
6. Ismael, NF (1982), Design of shallow rock-anchored foundations, Canadian Geotechnical Journal, Vol. 19, No. 2, pp. 463~471.
7. Littlejohn, GS (1992), Keynote lecture: Rock anchorage practices in civil engineering, Proc. Int. Symp. on Rock Supports in Min. and Underground Constr, Rotterdam, The Netherlands, pp. 257~268.
8. Littlejohn, GS and Bruce, DA (1977), Rock anchors-state of the art. Foundation Publications Ltd., Brentwood, Essex, England.
9. Saliman, R. and Schaefer, R. (1968), Anchored footings for transmission towers, ASCE Annual Meeting and National Meeting on Structural Engineering, Pittsburge, PA, Sept. 3~Oct. 4, Preprint 753, pp. 15~38.
10. Thomas-Lepine (2014), Rock bolts - improved design and possibilities, MSc Thesis Norwegian University of Science and Technology, Trondheim.
11. Xanthakos, PP (1991), Ground anchors and anchored structures, John Wiley & Sons, pp. 125~155.
12. You MK and Lee SD (2017), Pull-out resistance behavior of the anchor with the bump type resistors, Journal of the Korean geotechnical society, Vol. 33, No. 11, pp. 35~43.